The thermomechanical modeling of aluminothermic welds affected by different defects

Zakaria Mouallif, Bouchaib Radi, Ilias Mouallif

The thermomechanical modeling of aluminothermic welds affected by different defects

Z. MOUALLIF[a], B. RADI[a], I. MOUALLIF[b]

a. Laboratoire d'Ingénierie Mécanique, Management Industriel et Innovation, Faculté des Sciences et Techniques, Université Hassan 1er, Settat, Maroc
mouallifzakaria@gmail.com
b. Département de Génie Industriel et Productique, ENSAM, Université Moulay Ismail, Meknès, Maroc
i.mouallif@ensam.ac.ma

Summary:

This work is devoted to the analysis of the thermo-mechanical behavior of thermite welded rails by numerical simulation. A beam with the profile of an UIC60 rail and a weld in the middle, is simulated with the same function of an Hertzian pressure and with the same boundary conditions. For this purpose we present three welds: One without failures, the second one affected by porosity and the last one affected the defect of adhesion. In this modeling, we took the effect of the preheating of the rail ends into account. The preheating temperature generates residual stresses. The results are based on the shear stress SYZ in three parallel lines: The first (Z-1) and the last (Z+1) are positioned at the rail/weld interfaces and the second (Z0) is crossing in the middle of the weld.

Key terms: Finite elements; Shear stress; Welding; Aluminothermic; Defects; Porosity; Adhesion

1 Introduction

The assembly of the railway rails is usually made by a thermite welding process. This process involves fusion casting between the two ends of the rails which have to be joined [1,10]. The quality of this assembly is highly dependent on the conditions for the realization, which are generally difficult to achieve. Indeed, conventional control techniques for rails often prove the presence of various defects in the weld joint. According to different observations, bonding failures are a major defect of the railways in Morocco. This defect generates 75% of the cross breaks [4.9].

In order to better understand this phenomenon, we propose in this paper a 3D modeling of a rail beam with a thermite weld containing volume defects (porosity defects or defects of adhesion) and without defects. This modeling is done considering different forms. A spherical shape for porosity and a lack

of adhesion is represented by an empty space in the rail/welding interface. The shear stress was analyzed in the vicinity of these defects, using the finite element method.

2 Observation of the defects

By observations, we were able to classify the defects generated by the thermite welding process into two types: defect of adhesion (fig. 1-a) and of porosity (fig. 1-b).

The defect of adhesion (or bonding) is a major problem for the Moroccan railways. This defect generates 75% of the cross breaks in the rail/welding interface (this was confirmed by the ONCF), which could have been generated by an inadequate preheating [4].

At the moment of the execution of a weld, the imprisonment of gas during the molding process generates a defect on the filler metal, which is called the defect of porosity.

After a break, the affected welds were characterized by a great abundance of blister, giving the metal a "honeycomb"-appearance at the interior of the weld (fig. 1-b).
This fault is usually caused by the use of an insufficiently steamed mold [2].
Possible factors that could cause this type of defects are: insufficient preheating, climate change, execution errors, the presence of moisture in the mold, the crucible or thermite load.

(a)   (b)

Fig. 1. Defect of adhesion (a) and of porosity (b)

3 Wheel/rail contact

The first approaches concerning the behavior of the wheel/rail contact are a result of the studies by Hertz on the modeling of the contact of two metal cylinders with perpendicular axes rolling on one another. Hertz demonstrated that this contact is elliptical in shape [5].
This theory is easily transposable to the wheel/rail contact, because the rail's head is shaped almost cylindrically at the top and the wheel tread has a conical shape just like an "inclined" cylinder.
The modeling of the contact between the rail and the wheel is given in figure 2, where the Hertzian contact is elliptical in shape and the contact pressure is an ellipsoid of the maximum pressure P_0.
In this study we have considered the rail profile Vignole type UIC 60. The latter is defined by the NF A 45-317 [3] standard and the standard profile of the wheel with the diameter D = 920mm.

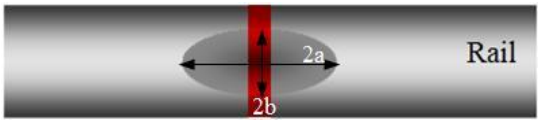

Fig. 2. Modeling of the wheel/rail contact [5-7]

The contact surface, analytically computed according to the approach of Hertz [2], in these conditions is a plane ellipse that is shown in figure 2.

The half axes a and b of the ellipse are calculated by the relations (1):

$$\frac{a}{m} = \frac{b}{n} = \sqrt[3]{\frac{3\pi}{2} \cdot \frac{(k_1 + k_2)}{\rho_1 + \rho_2^{'}} \cdot F_y} \qquad (1)$$

With: $\rho_1 (m^{-1})$ inverse of the transverse radius of the rail;

$\rho_2^{'} (m^{-1})$ inverse of the longitudinal radius of the wheel;

$k_1, k_2 (N^{-1} \cdot m^2)$ constants depending on Young's modulus E and Poisson's ratio ν of the steels of the wheel and the rail by the relation (2):

$$k_i = \frac{1 - \nu_i^2}{\pi \cdot E_i} \qquad \text{and} \qquad \cos(\tau) = \frac{\left|\rho_1 - \rho_2^{'}\right|}{\rho_1 + \rho_2^{'}} \qquad (2) \ \& \ (3)$$

a et b the large and small axis of the ellipse of contact;

m et n non-dimensional coefficients depending on the angle $\tau(°)$ defined by the equation (3);

$F_y (N)$ bearing force of the bodies in contact;

r non-dimensional coefficient.

Tab. 1. Coefficients in dependence of τ in degrees [2]

$\tau(°)$	10	20	30	40	50	60	70	80	90
m	6,61	3,78	2,73	2,14	1,75	1,49	1,28	1,13	1
n	0,32	0,41	0,49	0,57	0,64	0,72	0,80	0,89	1
r	2,8	2,3	1,98	1,74	1,55	1,39	1,25	1,12	1

The average pressure is calculable by dividing the force by the surface of the ellipse, as shown in the equation (4):

$$P_{moy} = \frac{F_y}{S} \qquad (4)$$

$S\ (m^2)$ surface of the ellipse ($S = \pi \cdot a \cdot b$)

The pressure at a point of the surface, depending on the x and z coordinates of that point, is calculable by the equation (5) [2,5]:

$$P(x,z) = \frac{3 \cdot F_y}{2 \cdot \pi \cdot a \cdot b} \cdot \sqrt{1 - \left(\frac{z}{a}\right)^2 - \left(\frac{x}{b}\right)^2} \qquad (5)$$

It is to notice, that the contact pressure is an ellipsoid.

The maximum pressure is obtained at the center of the ellipse for x = 0 and z = 0, by the equation (6):

$$P_0 = \frac{3 \cdot F_y}{2 \cdot \pi \cdot a \cdot b} = \frac{3}{2} \cdot P_{moy} \quad (6)$$

The contact being elliptical, the contact pressure is expressed by the equation (7):

$$P(x,z) = P_0 \cdot \sqrt{1 - \left(\frac{z}{a}\right)^2 - \left(\frac{x}{b}\right)^2} \quad (7)$$

4 Thermo-mechanical modeling

In this section, we considered a locomotive of 21.120 tons (2640 kg/wheel). This charge is equivalent to the tare weight of a TGV trailer. The contact surface is modeled by a Hertzian contact, as we have already developed in the paragraph above: The load applied in this simulation therefore is of the order of 505MPa [4,9].

The Vignola rail profile we considered is of the type UIC 60 [6-8]. The latter is defined by the standard NF A 45-317 [3].

By the observations of the defects, we modeled the following different cases:

- Defects of adhesion simulated by the existence of some form (not forming sharp angles), locating at the wheel/weld interface at the center of the pad [4,9].
- Porosity defects simulated by the existence of an abundance of spherical cavities (D=3mm) in the welded zone [4,9];

Subsequently, we considered an average Hertzian pressure of 505MPa.

By this modeling, we simulated the mechanical behavior of the rail subjected to an average Hertzian load of 505MPa, by means of the finite element method. In addition to this load, we considered the thermo-mechanical residual stress by a temperature change ($\Delta T = T_{réf} - T_{Fusion}$), with $T_{réf}$= 20°C (reference temperature) and T_{Fusion}= 600°C (temperature of the preheated rails' ends after merging of the thermite casting).

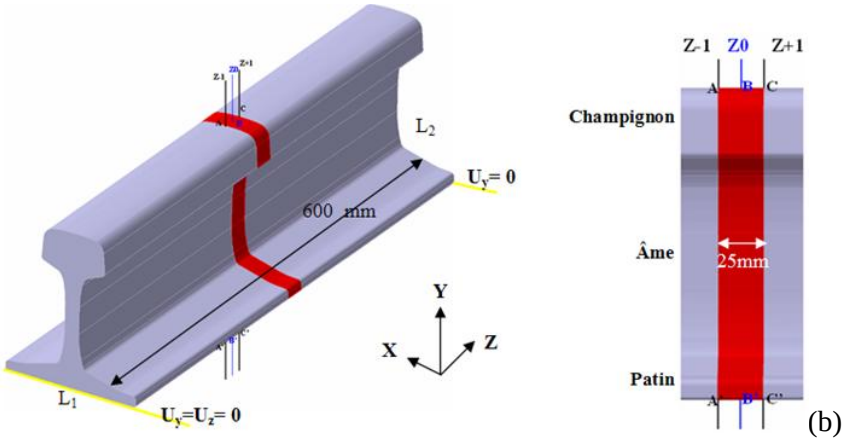

(a) (b)

Fig. 3. Geometric modeling and boundary conditions of a portion of the rail comprising a weld joint (a). Tracking in the plan (Y,Z) of the MB/ZF interfaces (Z+1 and Z-1) relative to the central axis (Z0) of the weld (b) [4,9].

Therefore, we considered a portion of the rail with a length of 0.6 m (fig. 3-a). This portion includes the limited welding zone between the position (Z-1) and (Z+1) as we have shown in (fig. 3-a). The width of this area is equal to 25mm (fig. 3-b).

The boundary conditions, that we have taken into account are: The displacements following Y and Z are zero on the line (L1) and only the displacement following Y is zero on the line (L2) (fig 3-a.).

In this modeling, we considered two configurations associated with the two defects mentioned above. In the first configuration, we assimilated the absence of adhesion at a recess of the material located in the central area of the pad. The geometric shape of this recess was determined by observations. In the second configuration, the defect of porosity was shown by spherical cavities with a diameter of 3mm, spread throughout the whole volume of the welding zone.

Both configurations were meshed with solid elements of the type SOLID 185. The selected mesh is fixed until the shear stress solution evolves no more in function to that size. Indeed, the refinement of the mesh allows us to develop our analysis with accurate results. The treated material is steel of the Young's modulus 200GPa for the rail and 243GPa for the welding. Poisson's ratio coefficient is taken equal to 0.3 [4].

5 Results and discussions

By the simulation of the studied structure (rail portion figure 3), we have sought to highlight the stress field developed by an average load.

Regarding this load and the considered boundary conditions, the behavior of this portion of the rail is that of a bending beam in the plane (Y,Z). This bending generates a shear stress due to the cutting force SYZ. In order to analyze this stress, we distinguish three scenarios: The first case is that of the defect-free structure. The second and third cases correspond respectively to the structures with poor adherence and defects of porosity.

In the first case (without default), the results we have obtained are illustrated by the graphics of figures 4 and 5.

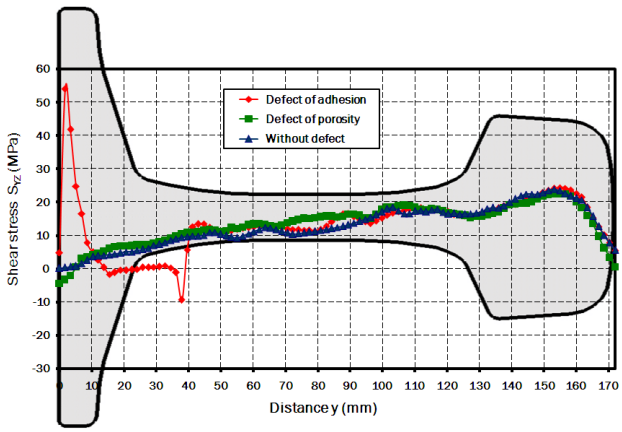

Fig. 4. Distribution of the shear stress SYZ in function of the distance y, along the vertical line Z-1

On the line Z-1, we can see that the defect in adhesion locally generated a disturbance of a shear stress field. Indeed, peaks have developed at the edges of this defect. The maximum value of this peak was obtained at the extreme bottom of de defect of adhesion and is of an order of 56MPa (fig. 4).

Regarding the defect of porosity, the disturbances of the stress field were not significant. Only the evolution of the SYZ component was characterized by small peaks, which were located along the whole heights of the rail and were of a generally small level.

On the line Z0, we can observe that the shear stress SYZ is more pronounced for a beam, that was affected by the defect of adhesion, than for the two other cases. This stress reaches a value of (~ −8MPa) and (~ 9MPa) at the extreme of the defect of adhesion. In contrast to this, we remark that the shear stress to the beam affected by the defect of porosity and the one just affected by the residual stresses that are generated by the thermal effect at the weld, annul themselves at the level of the pad and do not exceed the value (~ 2MPa) at the level of the core and the head of the rail (fig. 5-a).

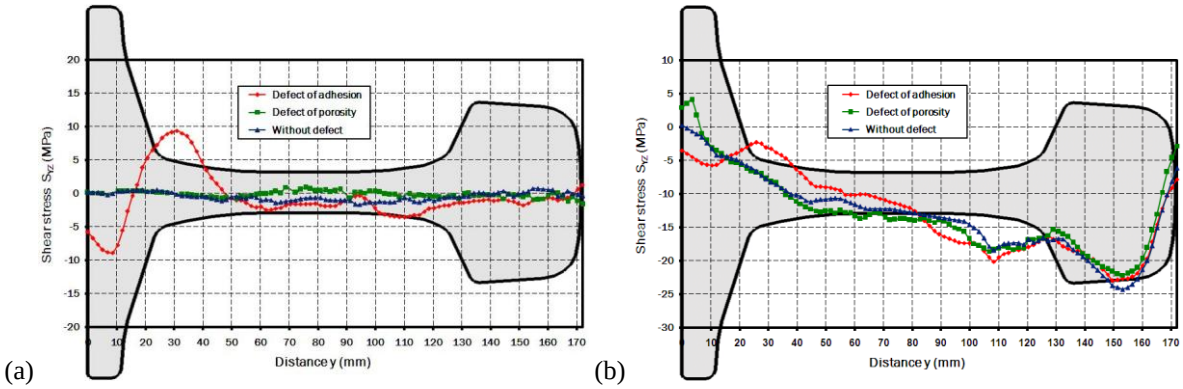

Fig. 5 Distribution of the shear stress SYZ in function of the distance y, along the vertical line Z0 (a), along the vertical line Z+1(b)

On line Z+1, we detect that the defect of adhesion has generated a small perturbation of the shear stress field in the vicinity of this defect. Concerning the defect of porosity, we notice a small variation along the entire height of the rail (fig. 5-b).

6 Conclusion

The objective of this work was to compare between a beam with a thermite weld without defects containing residual stresses due to the thermal effect during the execution of the weld, and those affected by the defect of porosity and a weld affected by the defect of adhesion. The results (finite elements) have allowed to observe the effects of the defects on the mechanical behavior at the rail/weld interfaces and in de middle of the weld. After analyzing these results, we found that the case of the defect of adhesion is more pronounced in the vicinity of the defect than the defect of porosity followed by the case without defects, but with a thermal excitation (the effect of the temperature of preheating). The shear stress SYZ is very important when the extreme of the defect of adhesion is near the free surface of the pad. On the other hand, this parameter attenuates rapidly to the other extreme of this defect, which is located far from the free surface of the pad. The presence of the defect of porosity

within the welding zone generates little peaks of shear stress at the extremes of each pore of this defect.

References

[1] P.-J. Mutton, E.-F. Alvarez, Failure modes in aluminothermic rail welds under high axle load conditions, Engineering Failure Analysis 11 (2004) 151–166.
[2] Jean-Claude ALACOQUE, Pierre CHAPAS, Transport ferroviaire: gestion de l'adhérence, pp. 6–8.
[3] NF A 45-317 Produits Sidérurgiques Laminés à Chaud, Rail Vignole type 60 kg/m et éclisse, Profil: caractéristiques et tolérance.
[4] I. Mouallif, A. Chouaf, A. Elamri, A. Benali, Effets des défauts de soudure aluminothermique sur le comportement mécanique des rails, Mechanics & Industry12 (2011) 343-351.
[5] I. Mouallif, A. Chouaf, A. Elamri, A. Benali, Étude du comportement mécanique des rails soudés par aluminothermie, VIème Journées d'Études Techniques 2010, Marrakech, Maroc, 2010.
[6] I. Mouallif, A. Elamri, A. Chouaf, A. Benali, Étude du comportement des rails soudés par aluminothermie, Communication au 3ème Congrès International Conception et Modélisation des Systèmes Mécanique CMSM'2009, Hammamet, Tunisie, 2009.
[7] I. Mouallif, A. Elamri, A. Chouaf, A. Benali, Étude du comportement mécanique des rails soudés par aluminothermie, Communication au 9ème Congrès de Mécanique, Marrakech, Maroc, 2009.
[8] I. Mouallif, A. Benali, A. Elamri, A. Chouaf, Étude du comportement des rails soudés par aluminothermie, Congrès Algérien de Mécanique CAM2009, Biskra, Algérie, 2009.
[9] I. Mouallif Z. Mouallif A. Benali F. Sidki, Finite element modeling of the aluminothermic welding with internal defects and experimental analysis , in: M. Belhaq and R . Ibrahim (́ed.), International Conference on Structural Nonlinear Dynamics and Diagnosis CSNDD'2012 (MATEC Web of Conferences1), EDP Sciences, Marrakech, Maroc, 2012.
[10] F. Sidki I. Mouallif M. Boudlal A. Elamri A. Benali, Experimental study of mechanical behavior and microstructural benchmarking between the rail and the thermite weld. International Journal of Engineering Research and Development, Vol 6 Issue 9 (2013), 53-58.